British Journal of Pharmacology (2007) 151, 63–74

0007–1188/07 $30.00
www.brjpharmacol.org

RESEARCH PAPER

NA^+- and K^+-channels as molecular targets of the alkaloid ajmaline in skeletal muscle fibres

O Friedrich[1,3], F v Wegner[1,3], M Wink[2] and RHA Fink[1]

[1]*Medical Biophysics, Institute of Physiology and Pathophysiology, University Heidelberg, Heidelberg, Germany and* [2]*Faculty of Biosciences, Institute of Pharmacy and Molecular Biotechnology, Ruprecht-Karls Universität Heidelberg, Heidelberg Germany*

Background and purpose: Ajmaline is a widely used antiarrhythmic drug. Its action on voltage-gated ion channels in skeletal muscle is not well documented and we have here elucidated its effects on Na^+ and K^+ channels.
Experimental approach: Sodium (I_{Na}) and potassium (I_K) currents in amphibian skeletal muscle fibres were recorded using 'loose-patch' and two-microelectrode voltage clamp techniques (2-MVC). Action potentials were generated using current clamp.
Key results: Under 'loose patch' clamp conditions, the IC_{50} for I_{Na} was 23.2 μM with Hill-coefficient $h = 1.21$. For I_K, IC_{50} was 9.2 μM, $h = 0.87$. Clinically relevant ajmaline concentrations (1-3 μM) reduced peak I_{Na} by ~5% but outward I_K values were reduced by ~20%. Na^+ channel steady-state activation and fast inactivation were concentration-dependently shifted towards hyperpolarized potentials (~10 mV at 25 μM). Inactivation curves were markedly flattened by ajmaline. Peak-I_K under maintained depolarisation was reduced to ~30% of control values by 100 μM ajmaline. I_K activation time constants were increased at least two-fold. Lower concentrations (10 or 25 μM) reduced steady-state-I_K slightly but peak-I_K significantly. Action potential generation threshold was increased by 10 μM ajmaline and repolarisation prolonged.
Conclusions and implications: Ajmaline acts differentially on Na^+ and K^+ channels in skeletal muscle. This suggests at least multiple sites of action including the S4 subunit. Our data may provide a first insight into specific mechanisms of ajmaline-ion channel interaction in tissues other than cardiac muscle and could suggest possible side-effects that need to be further evaluated.
British Journal of Pharmacology (2007) **151,** 63–74. doi:10.1038/sj.bjp.0707194; published online 12 March 2007

Keywords: skeletal muscle; ajmaline; loose-patch; sodium channel; potassium channel

Abbreviations: HERG, human ether-a-go-go-related gene; 2-MVC, two-microelectrode voltage clamp

Introduction

In skeletal muscle, ajmaline has been shown to block Na^+ currents in single intact frog skeletal muscle fibres (Körper *et al*., 1998). However, little is known about ajmaline effects on other voltage-gated ion channels, such as voltage-gated K^+ channels, in these preparations.

Ajmaline (Figure 1b) is of substantial clinical importance for its antiarrhythmic effects in life-threatening cardiac disorders like ventricular tachycardia (Manz *et al*., 1992; Todt *et al*., 1993) and to identify patients with increased risk for sudden death by Brugada's syndrome (Brugada *et al*., 2000; Keller *et al*., 2005). Despite its widespread clinical use, its molecular interactions with different ion channels are not well understood. In addition to its action as a Na^+-channel blocker in myocytes, Na^+ channel blocking by ajmaline has also been shown to be protective against anoxic injury in central nervous system white matter (Stys, 1995). Besides Na^+ channels, there is also evidence that ajmaline could act on other voltage- or ligand-gated ion channels. For example, in *Xenopus* oocytes, glibenclamide-sensitive K_{ATP} channels were blocked by ajmaline (Sakuta *et al*., 1992). K^+ currents mediated by cardiac human ether-a-go-go-related gene (HERG) channels expressed in *Xenopus* oocytes and human epidermal keratinocyte cells have been shown to be blocked by ajmaline to different extents. Contributions of HERG blockade to the antiarrhythmic action of the drug have been proposed (Kiesecker *et al*., 2004). In ventricular myocytes, ajmaline has also been shown to inhibit L-type Ca^{2+} currents (Enomoto *et al*., 1995; Bebarova *et al*., 2005b) and transient outward potassium currents (Bebarova *et al*., 2005a).

Although voltage-gated Na^+ channels are known to be molecular targets for many alkaloids (Wink, 1993, 2000),

Correspondence: Dr O Friedrich, Medical Biophysics, Institute of Physiology and Pathophysiology, University Heidelberg, Im Neuenheimer Feld 326, Heidelberg, 69120 Germany.
E-mail: oliver.friedrich@physiologie.uni-heidelberg.de
[3]These authors contributed equally to this work.
Received 14 July 2006; revised 16 November 2006; accepted 6 December 2006; published online 12 March 2007

not much is known about their possible alkaloid-binding sites. Alkaloid toxins alter voltage-dependent gating of Na^+ channels via binding to different intramembrane receptor sites (Cestele and Catterall, 2000). This has been proposed for the S6 subunit of domain I of Na^+ channels (Ragsdale *et al*., 1994; McPhee *et al*., 1994, 1995) and the positively charged voltage sensor of the S4 subunit (Butterworth and Strichartz, 1990). In voltage-gated Na^+ and K^+ channels the homologous S4 subunit (Figure 1a for Na_v^+ and K_v^+ channels) is highly conserved by the amino-acid sequences of Na_v domain IV (Popa *et al*., 2004) and K_v (e.g. Patel *et al*., 1997; Thornhill *et al*., 2003; Fleishman *et al*., 2004) found in skeletal muscle (Gutman *et al*., 2005). Because the S4 subunit also plays an important role in the fast Na^+ inactivation (Kra-Oz *et al*., 1992; Chen *et al*., 1996), it is of great interest whether alkaloids such as ajmaline affect the voltage-gated and time-dependent inactivation characteristics of fast Na^+ currents in skeletal muscle. Furthermore, if the S4 subunit were a pharmacological alkaloid-binding site, ajmaline would also be expected to block voltage-gated K^+ currents.

In the present study, we investigated the effects of ajmaline on the activation and inactivation of both Na^+ and K^+ currents in single intact amphibian skeletal muscle fibres.

Methods

Preparations

Single skeletal muscle fibres from the Mm. lumbricales of the frog *Xenopus laevis* were enzymatically isolated as described previously (Körper *et al*., 1998). All experiments were performed according to the guidelines laid down by the Local Animal Care Committee.

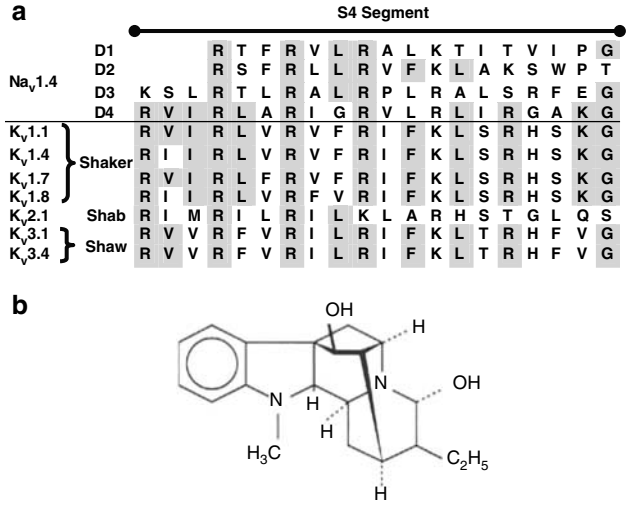

Figure 1 (**a**) Corresponding amino-acid sequences of the S4 subunit of the voltage-gated $Na_v1.4$ (Popa *et al*., 2004) and K_v family (Shaker: $K_v1.1$ from Thornhill *et al*., 2003; $K_v1.4$ from http://vkcdb.biology.ualberta.ca/; $K_v1.7$ from Kalman *et al*., 1998; $K_v1.8$ (see Yao *et al*., 1995); Shab: $K_v2.1$ from Patel *et al*., 1997; Shaw: $K_v3.1$ and $K_v3.4$ from http://vkcdb.biology.ualberta.ca/) found in adult skeletal muscle (Gutman *et al*., 2005). Homologous sequences between Na_v domains and K_v are highlighted in grey. (**b**) Chemical structure of ajmaline.

Solutions

Normal Ringer solution contained (mM): NaCl, 115; KCl, 2.5; $CaCl_2$, 1.8; $MgCl_2$, 1; *N*-2-hydroxyethylpiperazine-*N*′-2-ethanesulphonic acid, 5; pH 7.2. For two-microelectrode voltage clamp (2-MVC) recordings of I_K, 500 nM tetrodotoxin was added to the Ringer solution. Ajmaline (Sigma Chemicals, Taufkirchen, Germany) was added from a 1-mM stock solution to the desired concentration.

'Loose-patch' clamp experiments

Na^+ and K^+ currents (I_{Na} and I_K) were recorded using the 'loose-patch' clamp technique (Almers *et al*., 1983, 1984; Caldwell *et al*., 1986; Körper *et al*., 1998; Ruff, 1999; Rich and Pinter, 2003). Simultaneous patch clamp and intracellular microelectrode recordings were performed with a multiclamp amplifier (Molecular Devices, Sunnyvale, CA, USA). Patch pipettes and intracellular microelectrodes were pulled from borosilicate glass tubes (Science Products, Hofheim, Germany) with a horizontal puller (P87, Sutter Instruments, Novato, CA, USA) as described previously (Körper *et al*., 1998; Friedrich *et al*., 1999). For patch pipettes filled with Ringer solution, tip resistances were 0.2–0.4 MΩ and tip diameters 10–30 μm (see Figure 2). Penetrating sharp microelectrodes were backfilled with 3 M KCl and had resistances of 5–10 MΩ. A single muscle fibre was transferred to the recording chamber, mounted on the stage of an inverted microscope (IX70, Olympus, Germany) equipped with micromanipulators and the amplifier headstages. The microelectrode was softly driven into the fibre using an oil-driven micromanipulator (MHW-3; Narishige, Tokyo, Japan) until the membrane resting potential E_m could be monitored. The patch pipette approached the fibre membrane under visual control with a slight positive pressure applied to the tip. As Na^+ channel lateral distribution decreases towards the ends of muscle fibres (Almers *et al*., 1983; Caldwell *et al*., 1986), care was taken to record currents from patches in close proximity (~10–20 μm) to the end-plate region to maximize I_{Na} amplitudes. The pipette tip was softly pressed against the muscle membrane and the seal-resistance R_s monitored online by applying small (5–10 mV) alternating voltage steps. The seal-resistance represents a series circuit of the pipette resistance R_P and the membrane resistance R_m (Almers *et al*., 1983). The seal-resistance R_s was monitored throughout the experiments to calculate the correction

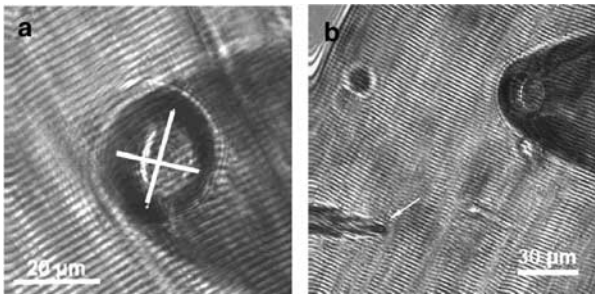

Figure 2 (**a** and **b**), Images of the tip of the 'loose-patch' pipette close to a muscle fibre. A sharp penetrating microelectrode (arrow in **b**) was used to continuously monitor resting membrane potential E_m.

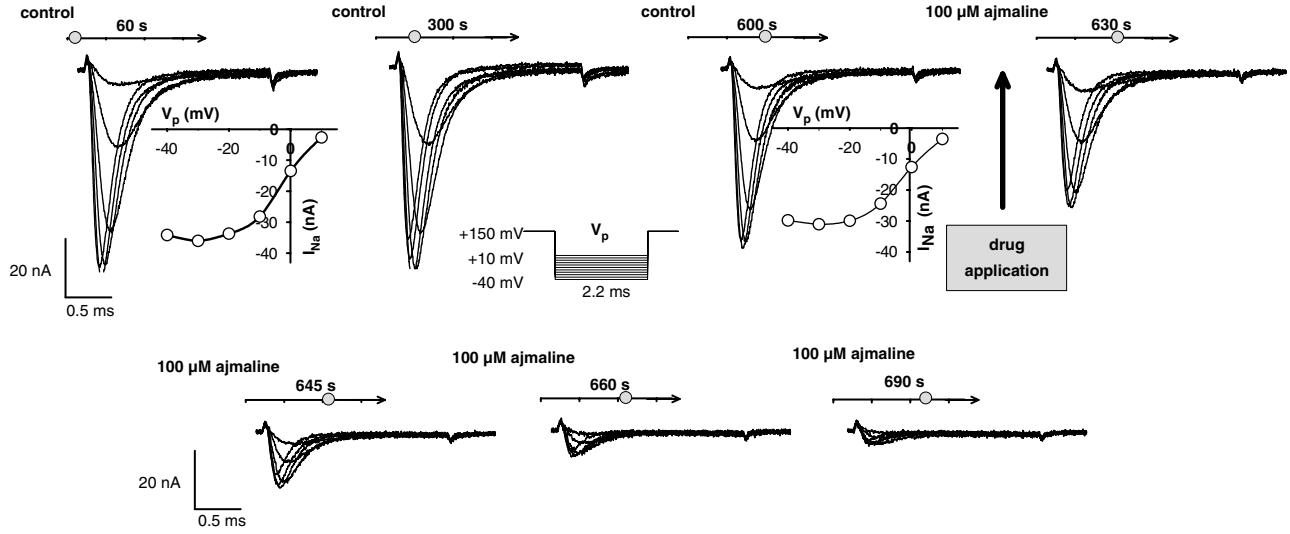

Figure 3 Stability of Na^+ current (I_{Na}) recordings and time course of ajmaline effect. For 10 min, a protocol to record I_{Na} traces was run every 30 s, showing stable I_{Na} amplitudes and I_{Na}–V relations. After addition of 100 μM ajmaline (arrow, at $\sim$600 s), current amplitudes quickly declined and inhibition was complete within $\sim$90 s. Seal resistance R_S: 2.2 MΩ, pipette resistance R_P: 324 kΩ, correction factor $A = 0.87$, resting membrane potential $E_m = -45$ mV. Note that the pulse protocol (inset) and the potential values of the I_{Na}–V plots shown correspond to the tip potential V_p rather than intracellular membrane potential.

factor $A = R_P/(R_P + R_S)$ for the tip potential V_p. The inverse relationship between seal-resistance and electrical noise in loose patches predicts improved signal detection for larger seal-resistance, especially in a low signal-to-noise environment (Hamill *et al*., 1981). It is therefore beneficial to obtain relatively large A factors, for example a fourfold increase in R_S over R_P ($A > 0.7$, Hong and Lnenicka, 1997; $A > 0.8$, Wang *et al*., 2001). Although smaller A values have been used, for A values less than 0.4, the leak usually cannot be adequately compensated (Rich and Pinter, 2003). In the present study, A was always larger than 0.8 (see also Körper *et al*., 1998). Results from experiments with more than 5% changes in A were discarded from analysis. V_p is the potential difference across the seal-resistance. Thus, the membrane patch potential E_{mp} has to be corrected by multiplication of the tip potential with A. To correlate E_{mp}, which is expressed relative to the extracellular reference electrode in the bath (i.e., bath potential set to zero), with the intracellular resting membrane potential E_m, the latter was monitored simultaneously with a sharp penetrating microelectrode near the patch pipette (see Figure 2). To verify the stability of the patches and to quantify the 'run-down' of ionic currents in our preparation, in a first series of experiments the same pulse protocol evoking nonlinear fast inward Na^+ currents (I_{Na}) was applied every 30 s. To make sure fibres were well repolarized, V_p was set to +150 mV. This corresponds to a holding potential of approximately −110 mV to −150 mV after conversion. From there, voltage steps (2.2 ms duration) were applied from −150 to +150 mV to the pipette tip (V_p) and the patch-current was recorded after low-pass filtering the data at 5 kHz ('activation protocol'). Fibres were repolarized to the holding potential for 1 s between pulses. To quantify the voltage-dependent fast inactivation of I_{Na}, a double-pulse protocol was applied: a first pulse of 25 ms duration to V_p between −160 and +160 mV was applied from a holding potential of +120 mV. After a short repolarization to 0 mV ($\sim$0.25 ms) the tip potential was set to a fixed value of −30 mV for 2 ms and the I_{Na} recorded ('inactivation protocol'). Experiments were performed at room temperature (20–22°C).

Assessment of drug effects

To test the time course of the inhibitory action of ajmaline on I_{Na} and I_K, 100 μM concentrations were applied to the bath solutions while recording complete sets of activation protocols in 15 s steps (see Figure 3, Results). Recording complete sets of I_{Na} also allowed detecting changes in the I–V relation, which would remain undetected when just using a fixed test pulse potential.

To test the concentration dependence of ajmaline steady-state inhibition on I_{Na} and I_K, activation and inactivation protocols were performed on single fibres before (control, I_0) and after the addition of single ajmaline concentrations (between 1 and 200 μM) to the bath solution, following an incubation time of 5 min (drug effect, I_5, see Results).

To directly compare the inhibitory ajmaline effects on I_{Na} and I_K between individual preparations, the fraction I_5/I_0 was used instead of calculating the surface-normalized currents, which contain uncertainties of up to 15% from the determination of the patch pipette diameter in the transmission light microscope. Therefore, I_5/I_0 represents a more reliable parameter for the drug effect.

2-MVC experiments

As the time course of I_K at more positive potentials and prolonged durations is difficult to record with the 'loose-patch' clamp technique owing to contributions from uncontrolled membrane beneath the rim (Almers *et al*., 1983), the '2-MVC' technique (Friedrich *et a*l., 1999, 2002, 2004) was used to investigate the ajmaline effect on the

activation and inactivation of delayed outward I_K. The 2-MVC technique is especially suitable to record whole-cell I_K under maintained depolarization (Friedrich *et al*., 2002). Single fibres were clamped to an intracellular holding potential of –90 mV and depolarizing potential steps (200–300 ms duration) of 10 mV increments were applied. The amplitudes of I_K were analysed before (control) and 5 min after the addition of ajmaline. Under control conditions, I_K shows time-dependent inactivation for more positive depolarizations, which was quantified by the steady-state-I_K to peak-I_K ratio. To quantify the time course of K^+ channel activation, the I_K traces were fitted to an n^4 kinetics as described for rat muscle (Beam and Donaldson, 1983). To record action potentials, the 'current clamp' mode of the voltage clamp amplifier was used. Single fibres were pre-set to a membrane potential of −90 mV by injection of a constant current. Current pulses of 1.5 ms duration were then applied in 100 nA steps to determine the action potential threshold. Thresholds were compared in the same fibre under control conditions and after the addition of ajmaline for 5 min. Trains of action potentials were elicited in a series of four consecutive action potentials at ~20 ms intervals and the post-train period recorded. This protocol is suitable to investigate changes in the excitability of resting fibres, for example, owing to ajmaline-induced hypo-/hyperexcitability as well as a possible use dependence of ajmaline. In a third set of experiments, a double-pulse protocol with varying recovery intervals was used to elicit two action potentials sequentially. From the decrease of amplitude with decreasing recovery interval, the refractory period and the recovery from inactivation can be estimated (Friedrich *et al*., 2004).

Data analysis

From the 'loose-patch' activation protocols on I_{Na} and I_K, *I–V* curves were reconstructed from the peak I_{Na} amplitude and the apparent 'steady-state' I_K amplitude at 2 ms after correcting the tip potential for the pipette resistance. Steady-state activation and inactivation curves for I_{Na} were reconstructed as described before (Catterall, 1988; Körper *et al*., 1998; Friedrich *et al*., 1999; Desaphy *et al*., 2001; Rich and Pinter, 2003). The curves were fitted with Boltzmann fits yielding a half-activation potential $m_{0.5}$, half-inactivation potential $h_{0.5}$ and slope factors *k*. From the mean values of $m_{0.5}$, $h_{0.5}$ and *k* from activation and inactivation, idealized h_∞ and m_∞ curves were recalculated for each drug concentration used. Control values were placed together after testing for no significant differences between batches and idealized appropriate control curves were reconstructed (see Results).

Drug effects were assessed using paired *t*-tests on single fibres, where complete data sets of before/after drug application recordings were available. $P<0.05$ was considered significant. Paired tests included Student's *t*-test or Wilcoxon signed-rank tests when normality failed (SigmaPlot 9, Systat Software, Point Richmond, CA, USA).

Dose–response curves for the inhibition of I_{Na} and I_K amplitudes by ajmaline were obtained by least-square Hill fits to the I_5/I_0 data (SigmaPlot 9). From these curves, the mean concentration for 50% blocking (IC_{50}) and the slope factor *h* (Hill coefficient; see Körper *et al*., 1998) could be extracted.

Results

Stability of the 'loose-patch' clamp recordings and time course of ajmaline effects

Figure 3 shows a series of repetitive recordings of I_{Na} with the 'loose-patch' clamp technique in a representative single muscle fibre: 2.2 ms lasting potential step pulses to the pipette tip were applied from a V_p of +150 mV to values ranging from $V_p=-40$ mV to $V_p=+10$ mV as shown in the inset. The protocol was repeated every 30 s for 10 min under control conditions to verify the stability of the technique and to estimate possible contributions from 'run-down' of the channels to the drug effect. The first three recordings at 60, 300 and 600 s together with the corresponding *I–V* plots clearly validate the stability of the patch under control conditions, that is, no significant run-down or shift in the *I–V* curve was seen for at least 10 min. At 600 s, 100 μM ajmaline was added to the bath solution and recording protocols of I_{Na} were performed every 15 s. The following four recordings showed that the inhibition of I_{Na} was almost complete after 90 s. A detailed analysis of the *I–V* relation of I_{Na} before and after the addition of ajmaline to the bath solution is shown in Figure 4 for another single fibre. Figure 4a shows that the patch is stabilized 1 min after patch formation and remains stable for the remaining time. Figure 4b shows the fast kinetics of inhibitory ajmaline action on I_{Na}, which predominantly affects peak current amplitude $I_{Na,peak}$ and also shifts *I–V* relations to some minor extent. Figure 4c shows the time course of $I_{Na,peak}$ inhibition by 100 μM ajmaline, which is complete after ~3 min. Therefore, 'loose-patch' recordings at 5 min reflect a steady-state inhibition of I_{Na} (Figures 3 and 4) and I_K (not shown). To be able to study the steady-state activation of I_{Na}, a complete pulse protocol was applied to the fibres before and 5 min after the ajmaline application (see below). Peak I_{Na} density normalized to the apparent membrane patch area derived from the pipette diameter was calculated for all fibres under control conditions. Values ranged from −1.5 to −15 mA/cm^2 in 36 single fibres (mean ± s.e.m. −4.6 ± 0.5 mA/cm^2).

Concentration dependence of I_{Na} and I_K inhibition by ajmaline

Figure 5a shows recordings of I_{Na} and early I_K measured with the 'loose-patch' clamp technique in Ringer solution before (control) and 5 min after the application of 25 μM ajmaline (middle panel). Note that depolarizations were larger compared with the protocol in Figure 3 to induce the outward I_K. Under our experimental conditions (amphibian muscle, room temperature), inactivation kinetics of I_{Na} is very fast, that is, I_{Na} can be considered almost completely inactivated after 1 ms (see Figure 2a in Körper *et al*., 1998). Therefore, contaminating contributions of inward I_{Na} to the outward 'steady-state' I_K can be considered negligible. On the other hand, as the activation time constants of I_K for negative membrane potentials is in the range of 5 ms (see

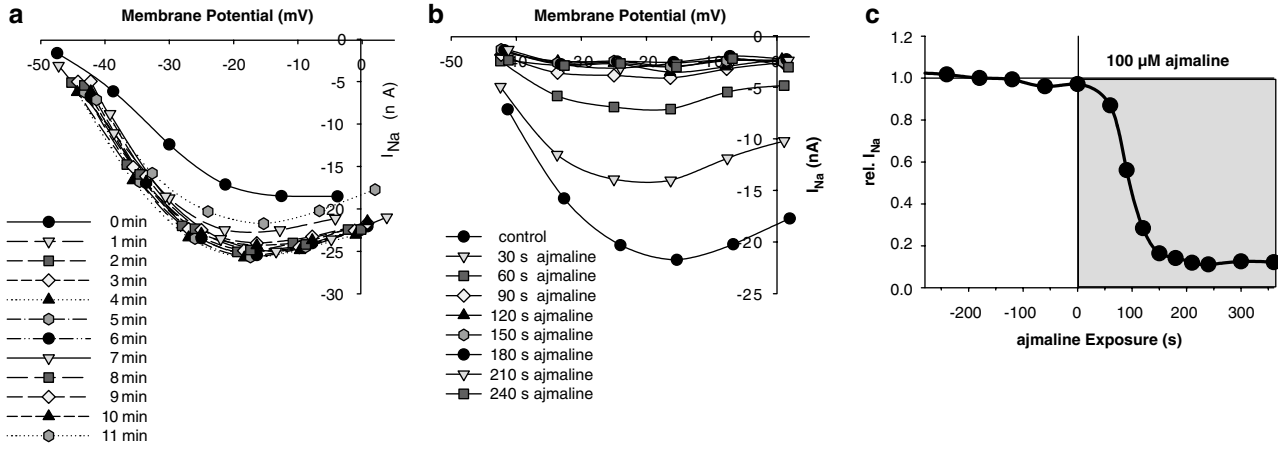

Figure 4 Time and voltage dependence of I_{Na} during a 10-min control period (**a**) and following addition of 100 μM ajmaline in another single fibre. I_{Na}–V plots are shown after conversion of the applied tip potential to intracellular membrane potentials as described in the Methods. Ajmaline affects both peak amplitudes (**c**) and (**b**) voltage dependence of I_{Na}.

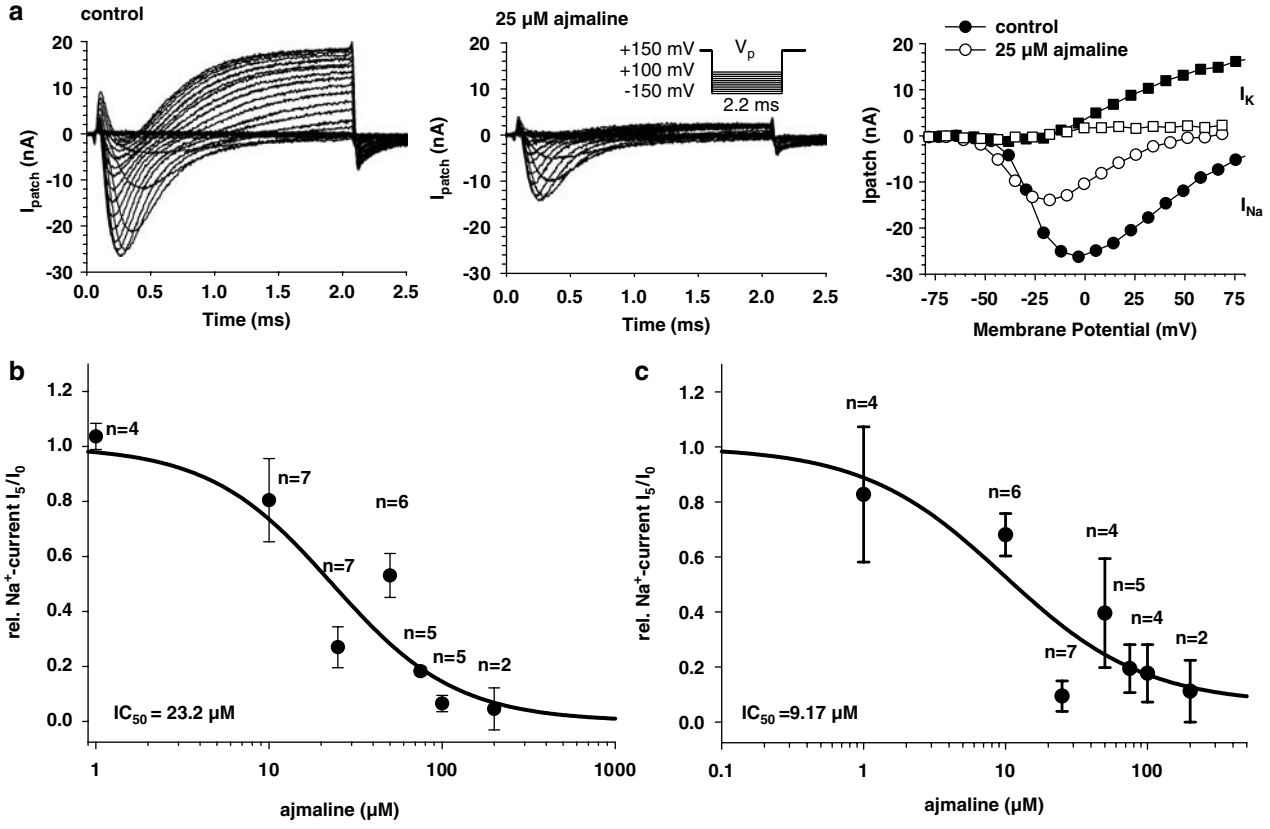

Figure 5 Concentration dependence of I_{Na} and I_K blocking with the 'loose-patch' clamp technique. (**a**) Recordings of I_{Na} and I_K before (left panel, R_S: 2.0 MΩ, R_P: 288 kΩ, $A = 0.87$, $E_m = -47$ mV) and after the addition of 25 μM ajmaline (middle panel, R_S: 1.8MΩ, R_P: 288 kΩ, $A = 0.86$). The right panel shows the corresponding I–V relations. (**b**) Concentration dependence of relative peak I_{Na} inhibition by ajmaline. (**c**) Concentration dependence of relative 'steady-state' I_K inhibition by ajmaline. IC_{50} values derived from Hill fits are indicated. Error Bars are s.e.m. with n single fibres (paired data).

Figure 8d below) there is also no significant contribution of outward I_K to the maximum peak inward I_{Na}.

Following incubation with 25 μM ajmaline, I_{Na} was reduced to approximately 50% whereas inhibition of I_K was more pronounced. The right panel of Figure 5a shows the corresponding I–V plots for peak I_{Na} and 'steady-state' I_K, respectively. The I_{Na}–V plots were rescaled to intracellular membrane potential. As can be seen, there was some leftward shift of the I_{Na}–V relation by ajmaline. The concentration dependence of the ajmaline effect on relative I_{Na} inhibition (I_5:I_0) and I_K inhibition (estimated from the slope of the I_K–V plots at 0 and 5 min) is shown for several

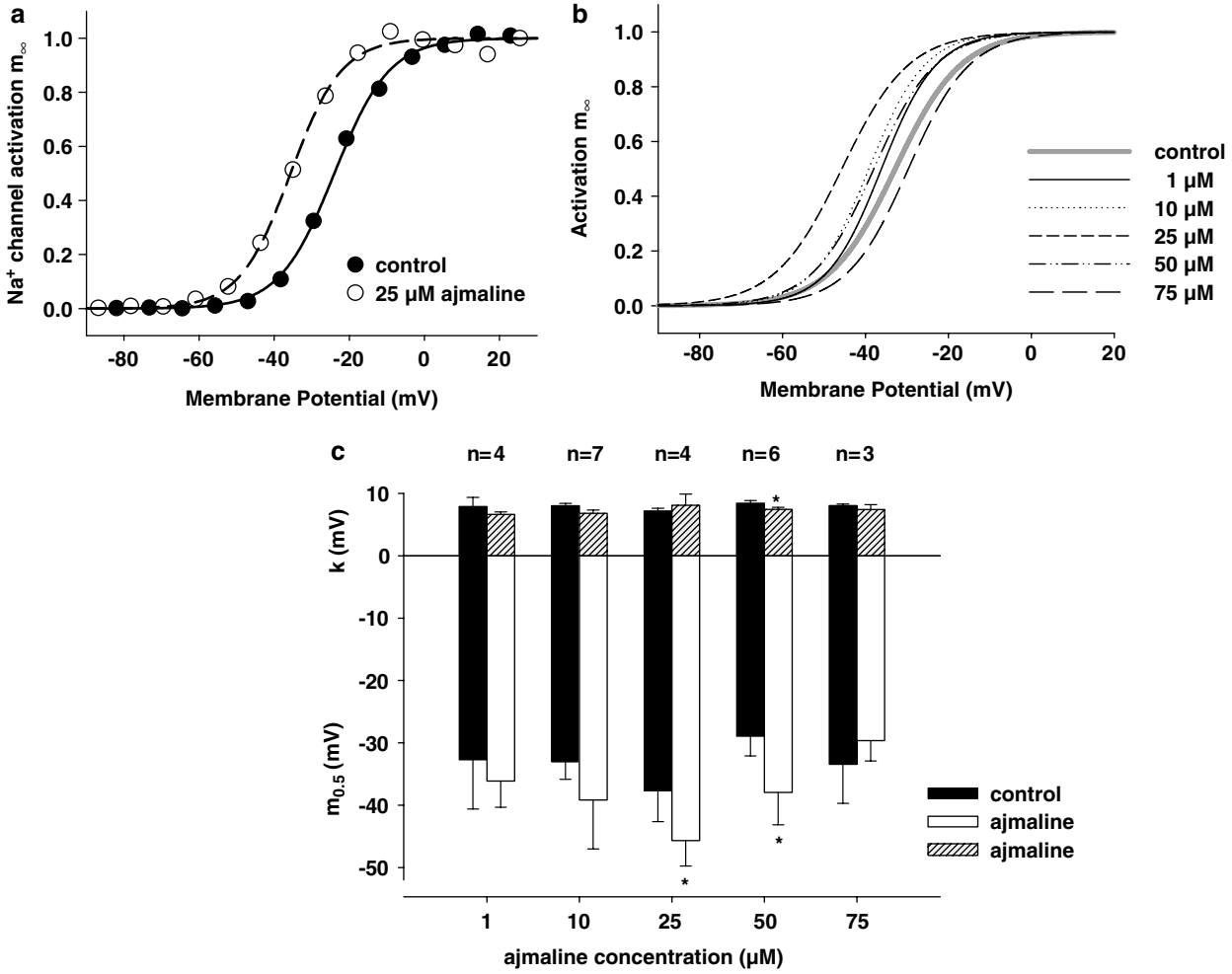

Figure 6 Ajmaline effects on steady-state activation of I_{Na}. (**a**) m_∞ curve derived from the I_{Na}–V relation of the fibre shown in Figure 5a before (control: filled circles) and after the addition of 25 μM ajmaline (open circles). (**b**) Idealized m_∞ curves reconstructed from the mean $m_{0.5}$ and slope factors k of Boltzmann fits derived from recordings as shown in (**a**). (**c**) Summary of $m_{0.5}$ and k values for the different ajmaline concentrations (white or shaded bars, respectively) and their corresponding controls (black bars). *$P<0.05$. Error Bars: s.e.m.

fibres in Figure 5b and c, respectively. A Hill fit to the data (solid lines) revealed an IC_{50} value of 23.2 μM ($r^2=0.94$) for the inhibition of I_{Na} and 9.17 μM for I_K ($r^2=0.91$). The Hill coefficients were $h=1.21$ and 0.87, respectively. It is interesting to note that ajmaline inhibition of currents did not appear to be use dependent. A single set of stimuli applied 5 min after ajmaline incubation resulted in the same level of inhibition compared with repetitive stimulation (compare Figure 5a and Figure 4c for 100 μM ajmaline).

Effects of ajmaline on voltage-dependent I_{Na} *activation and fast inactivation*

Figure 6a shows the steady-state Na^+ channel activation curve m_∞ obtained from the I_{Na}–V plot of the fibre shown in Figure 5a under control conditions and after the addition of 25 μM ajmaline. Also shown are the corresponding Boltzmann fits to the data. For the fibre shown, the half-activation potential $m_{0.5}$ was -23.9 mV under control conditions and -35.6 mV after incubation with 25 μM ajmaline. The slope factors k were 7.3 and 6.8 mV, respectively. From the $m_{0.5}$ and k values of several fibres, average Boltzmann fits were reconstructed for each ajmaline concentration used (Figure 6b). As all control values were not significantly different ($m_{0.5}$: $P>0.75$, k: $P>0.76$), they were placed together to reconstruct one average fit representative for all controls (solid grey line in Figure 6b). For all controls, $m_{0.5}$ was -32.8 ± 1.9 mV and $k=7.9\pm0.3$ mV ($n=24$). Interestingly, as seen in Figure 6b, ajmaline concentrations up to 25 μM induced a leftward shift of the activation curve (e.g., at 25 μM ajmaline: $m_{0.5}=-45.7\pm4.1$ mV and $k=8.1\pm1.8$ mV, $n=4$), whereas higher concentrations, 50 μM, seemed to induce a plateauing of the ajmaline effect followed by a marked rightward shift at 75 μM. However, this finding might be affected by the already reduced signal-to-noise ratio starting from 50 μM and should be interpreted with caution. For 100 and 200 μM, activation curves could not be robustly assessed because of the almost complete inhibition of I_{Na}, preventing the construction of I_{Na}–V plots. Figure 6c shows the paired results (control vs ajmaline) in several fibres at the concentrations indicated.

Fast steady-state voltage-dependent inactivation of I_{Na} derived from double-pulse protocols are summarized in Figure 7. Figure 7a shows recordings from a representative

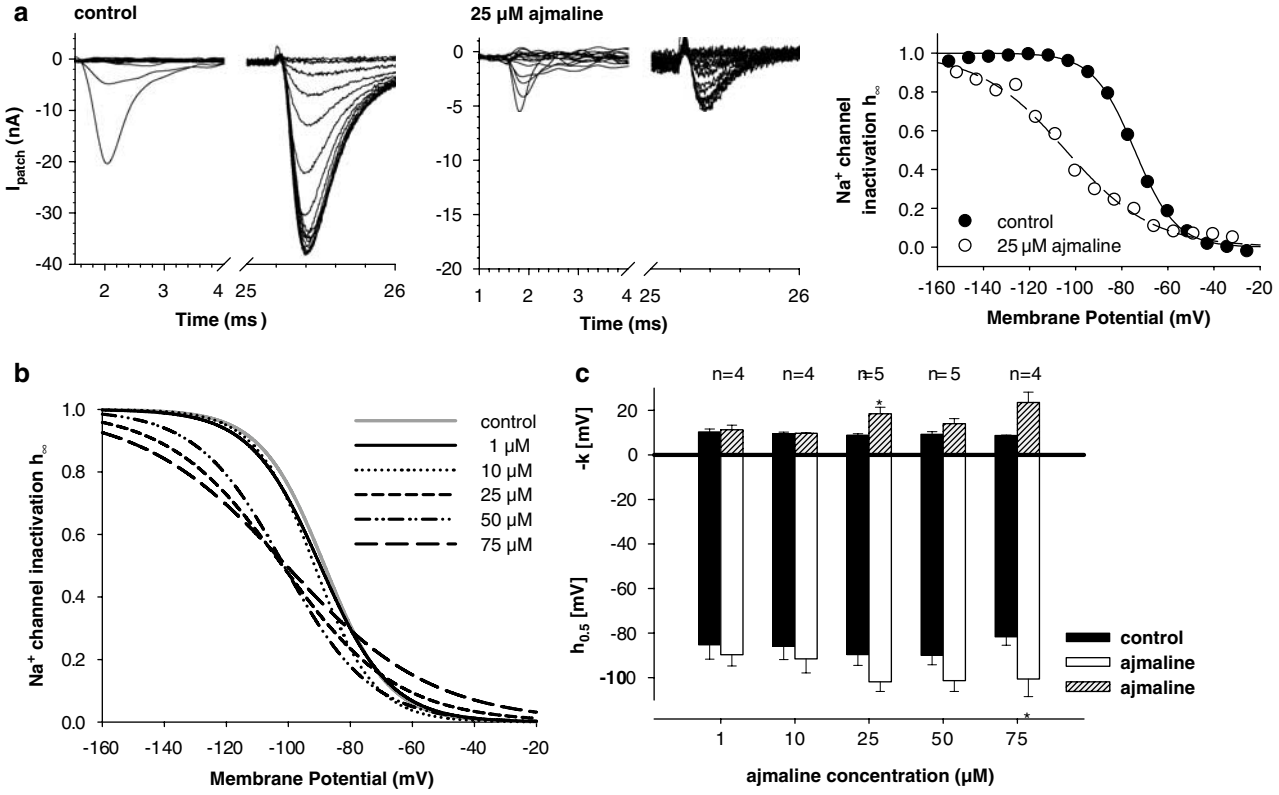

Figure 7 Ajmaline effects on steady-state inactivation of I_{Na}. (**a**) Original recordings of I_{Na} from double-pulse protocols before and after the addition of 25 μM ajmaline (R_S: 1.8 MΩ, R_P: 290 kΩ, A = 0.86, $E_m = -45$ mV). Note the different scaling of the ordinate in (**a**) and (**b**). The h_∞ curve was calculated as described in the Methods and fitted by a Boltzmann fit (right panel). Ajmaline shifted the h_∞ curve to the left and flattened its slope. (**b**) Idealized h_∞ curves for different ajmaline concentrations reconstructed from mean $h_{0.5}$ and k values as shown in (**c**). *$P <$ 0.05. Error Bars: s.e.m.

single fibre under control conditions and following 25 μM ajmaline incubation. The right panel shows the *I–V* relation for the peak I_{Na} during the test pulse relative to its maximum I_{Na}. This steady-state Na^+ channel inactivation curve, h_∞, reflects the availability of Na^+ channels at a given membrane potential (Pappone, 1980; Almers *et al*., 1983). From the Boltzmann fits to the data, a half-inactivation potential of −74.4 (control) and −104.3 mV (25 μM ajmaline) was calculated. The slope factors were −8.9 and −18.7 mV, respectively. As for I_{Na} activation, average idealized inactivation curves were reconstructed for each ajmaline concentration (Figure 7b). The control values for $h_{0.5}$ ($P > 0.85$) and k ($P > 0.75$) were not significantly different and were combined ($h_{0.5} = -88.3 \pm 1.6$ mV and $k = -10.3 \pm 0.5$ mV, $n = 33$) to reconstruct a representative control h_∞ line (grey line in Figure 7b). Ajmaline shifted the h_∞ curves to the left and flattened their slope (e.g., at 25 μM ajmaline: $h_{0.5} = -101.8 \pm 4.4$ mV and $k = -18.5 \pm 2.9$ mV, $n = 5$). This is summarized in Figure 7c for the paired control vs ajmaline data on h_∞ in several single fibres.

Ajmaline effects on the delayed I_K *outward currents*

To be able to investigate outward potassium currents, I_K, under maintained depolarization, 2-MVC recordings were carried out. Figure 8a shows I_K recordings in a single fibre before (control) and after the application of 100 μM ajmaline. Under control conditions, fibres always showed inactivation of I_K for larger depolarizations after reaching a maximum amplitude at ~20 ms, as can be seen in the example shown. The ratio of steady-state I_K to peak I_K is summarized for seven single fibres in Figure 8b (filled circles, control) over the whole potential range tested. Interestingly, after addition of 100 μM ajmaline, both steady-state and peak I_K were markedly suppressed, as shown in the example and in Figure 8b and c. Some fibres did not even reach the maximum I_K amplitude at the end of the ~200 ms pulse. The activation time constant τ_{act} for K^+ channel activation was significantly larger after addition of 100 μM ajmaline compared with controls ($P < 0.001$, Figure 8d). Lower concentrations of ajmaline showed less prominent effects. For 10 μM, steady-state-I_K and peak-I_K were almost unchanged (not shown). For 25 μM, the effect on steady-state-I_K reduction was already significant although small (Figure 8c, $P < 0.02$ in three out of four fibres). On the other hand, peak-I_K reduction was already marked as shown by the increase in the ratio of steady-state-I_K to peak-I_K (Figure 8b).

Ajmaline effects on action potential properties

To quantify the blocking effects of ajmaline on Na^+ and K^+ currents seen under voltage clamp conditions on action potential properties, current clamp experiments were performed. Figure 9a shows the time course of membrane

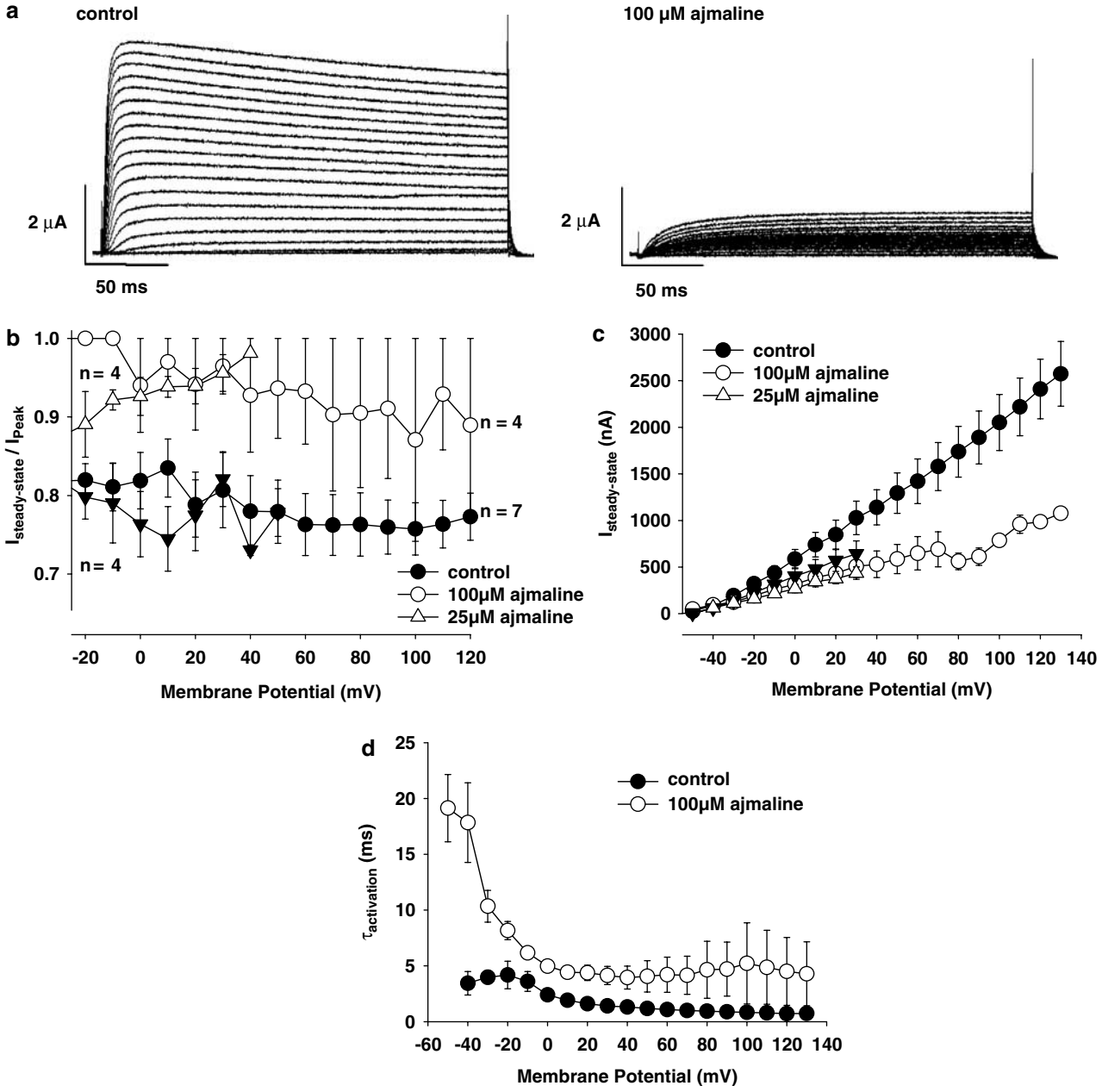

Figure 8 Ajmaline effects on K^+-currents (I_K). (**a**) I_K recorded with the 2-MVC technique in a representative single muscle fibre before (left) and after the application of 100 μM ajmaline (right). Test pulses ranged from -50 to $+130$ mV. (**b**) Control fibres showed approximately 20% inactivation of I_K under maintained depolarization, as judged from the steady-state to peak-I_K amplitude ratio, whereas ajmaline greatly reduced this amount of inactivation both for 100 μM (circles) and 25 μM (open triangles; filled triangles: corresponding controls). (**c**) After addition of 100 μM ajmaline, steady-state I_K amplitudes were reduced to $\sim$40% of controls, especially for larger depolarizations. The effect was less pronounced but significant for 25 μM ($P<0.02$, three out of four fibres). (**d**) Ajmaline (100 μM) significantly increased the time constants of K^+ channel activation ($\tau_{act.}$) compared to controls. Error Bars: s.e.m.

potential in a representative single fibre held at -90 mV and depolarized by step pulses of $\sim$1.5 ms duration and increasing amplitude under control conditions (left) and following incubation at 10 μM ajmaline (middle). Ajmaline increased the threshold for action potentials about 100 nA and decreased their amplitude about 60 mV. The blocking of repolarizing K^+ currents was quantified by the exponential decay of the action potential and yielded time constants that were about fourfold increased for 10 μM ajmaline and about 12-fold increased for 100 μM ajmaline (right panel). To assess any hyperexcitability effects of ajmaline on muscle fibres under repetitive stimulation conditions, a train of four repetitive action potentials was elicited at $\sim$20 ms intervals (Figure 9b). Ajmaline decreased excitability also under these experimental conditions rather than inducing excessive generation of action potentials. As a measure for the refractory period, double-pulse protocols were used to elicit two action potentials in a sequence. Figure 9c shows that

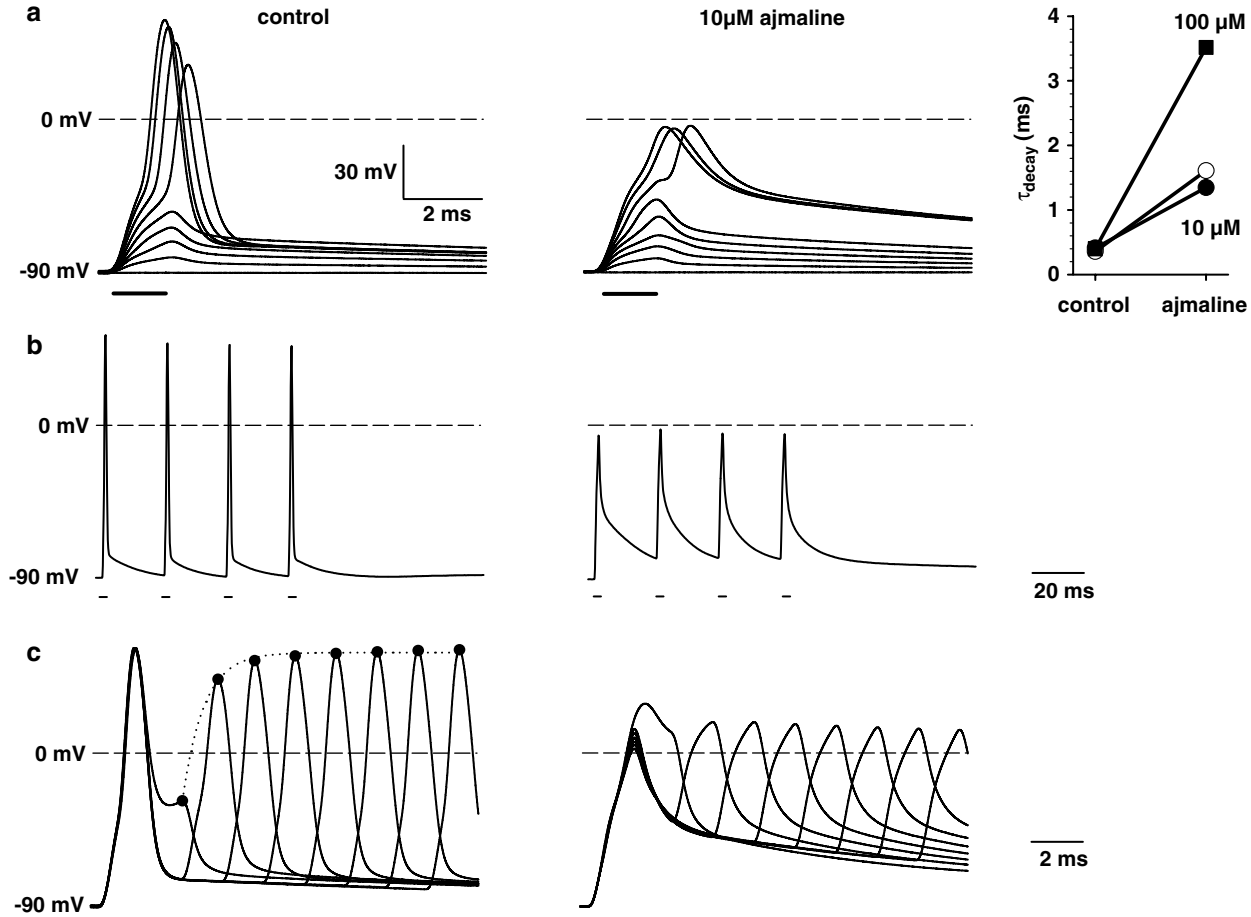

Figure 9 Ajmaline effects on action potentials. (**a**) Membrane potentials recorded with the current clamp technique in a representative single muscle fibre before (left) and after the addition of 10 μM ajmaline (middle). Current pulses were increased in 100 nA steps of $\sim$1.5 ms duration. The threshold was shifted 100 nA towards larger currents after ajmaline addition. The right panel shows the increase in the decay time constant with ajmaline concentration from some single fibres. (**b**) Repetitive action potentials did not produce any hyperexcitability (i.e., generation of action potentials in the post-train period) after 10 μM ajmaline. (**c**) Double-pulse stimulation of action potentials shows a normal reduction in action potential amplitude when the second action potentials is elicited shortly after the first under control conditions but almost no reaction after addition of 10 μM ajmaline.

under control conditions, as the interval between the two action potentials decreased, the amplitude of the second decreased in an exponential way. Because of the blocking effect of ajmaline on Na^+ channels, longer recovery intervals could not further increase action potential amplitudes.

Discussion

We have previously shown that the skeletal muscle SCN4A Na^+ channel is a target for alkaloids (Körper *et al*., 1998). In the present study, we extended our investigation of ajmaline effects on voltage-gated I_{Na} also to I_K. In skeletal muscle, voltage-gated K^+ channels are mostly represented by the KCNA family, part of the K_v family (see Gutman *et al*., 2005, for International Union of Pharmacology nomenclature; formerly known as K_A^+ channels, see Catterall, 1988), which show the typical channel structure features with voltage sensor S4, toxin-binding sites and a single ion-conducting pore (Lehmann-Horn and Jurkat-Rott, 1999). Additionally, the S4 segment of voltage-gated ion channels represents a highly conserved homologous repeat (Butterworth and Strichartz, 1990; Catterall, 1992; see also Figure 1a).

In our skeletal muscle preparation, ajmaline blocked I_{Na} and I_K in the 'loose-patch' setting with an apparent IC_{50} of $\sim$23 and $\sim$9 μM, respectively. This suggests a higher susceptibility of K^+ channel blocking by ajmaline compared with Na^+ channels. In the range of clinically relevant plasma concentrations of 1–3 μM unbound ajmaline (Kiesecker *et al*., 2004), this corresponds to approximately 20% blockade of repolarizing K^+ currents but only a minor block of I_{Na} (5–10%, Figure 5). This combination of effects might suggest hyperexcitability for lower concentrations of ajmaline (e.g., 10 μM) in skeletal muscle in agreement with the pro-arrhythmic potency of the drug, sometimes seen in cardiac muscle. However, in single skeletal muscle fibres, we could not detect any hyperexcitability induced by the lower ajmaline concentrations of 10 μM. There were no signs for continuing action potential activity following repetitive stimulation. In particular, the threshold for action potentials was increased by ajmaline and the decay phase of the action

potential prolonged in agreement with our findings on the blocking effect of ajmaline on both channels. This suggests either different binding sites or other, yet unknown differences in the mode of ajmaline action in heart and skeletal muscle.

Our IC_{50} values for I_{Na} are in good agreement with recent data from rat ventricular myocytes. Bebarova *et al*. (2005b) found an IC_{50} of $\sim 27\,\mu M$. The same authors reported IC_{50} values for ajmaline inhibition of cardiac transient outward K^+ currents (I_{to}) of $\sim 25\,\mu M$, which is considerably larger than our values in amphibian skeletal muscle voltage-dependent I_K under 'loose-patch' conditions. However, when calculating the association and dissociation rate constants for ajmaline-dependent I_{to} inactivation, the authors found a K_d value of $\sim 4.5\,\mu M$ (Bebarova *et al*., 2005a). The difference in IC_{50} and K_d was compatible with Hodgkin–Huxley simulations, suggesting an open channel blocking mode of ajmaline action on I_{to} in mammalian ventricular myocytes. Our results, with a much smaller IC_{50}, indicate that this might not be the case for skeletal muscle I_K. Further studies are necessary to evaluate the exact nature of the ajmaline effect on K^+ channel gating behaviour in skeletal muscle.

Ajmaline showed a marked voltage-dependence on steady-state fast channel activation and inactivation. Na^+ channel activation, m_∞, was concentration-dependently shifted towards hyperpolarized potentials for concentrations up to $50\,\mu M$. This leftward shift accounted for approximately –13 mV at $25\,\mu M$. Around $50\,\mu M$, this effect seemed to plateau and, for $75\,\mu M$, this effect was reversed and a rightward shift became apparent, suggesting a bimodal mode of action of ajmaline on channel activation gating. The voltage sensitivity of channel gating represented by the slope of m_∞ was almost unaltered. For I_{Na} fast inactivation, the leftward shift of h_∞ was unimodal and increased with ajmaline concentration, that is, $h_{0.5}$ was shifted almost by –20 mV at $75\,\mu M$. Additionally, ajmaline markedly reduced the steepness of the inactivation curves, thus reducing voltage sensitivity. The changes in gating behaviour can only partially explain the reduction in Na^+ current density by ajmaline. For example, at a given resting membrane potential of -75 mV, the flattened inactivation curve would partially compensate for the reduced availability induced by the leftward shift of the curve alone. As the method presented here reflects the relative change in current densities induced by ajmaline, it seems possible that ajmaline functionally knocks out Na^+ channels within the patch, thus reducing current density to a larger extent as expected from the changes in gating of the remaining Na^+ channels alone (Friedrich *et al*., 2006).

Our data on I_K, using the 2-MVC on a longer time scale and more positive potentials, support those obtained with the 'loose-patch' clamp technique. The latter is known to be less stable under such conditions (Almers *et al*., 1983). Ajmaline effectively blocks not only voltage-gated Na^+ currents but also K^+ currents in frog skeletal muscle fibres. Interestingly, when comparing our 'loose-patch' data on I_K blocking of ajmaline to those obtained under prolonged depolarizations using the 2-MVC technique, ajmaline seems to block early I_K components with a higher potency than late steady-state I_K after several 100 ms. In particular, $100\,\mu M$ ajmaline showed clear effects, whereas for $25\,\mu M$ of ajmaline effects on steady-state I_K were much smaller. This lower concentration, however, already strongly reduced the early peak I_K. This suggests differential affinities of ajmaline towards different K_v families expressed in skeletal muscle (see Figure 1a). Among those, $K_v1.1$, $K_v1.4$, $K_v1.7$, $K_v1.8$ and $K_v3.1$ show fast activation kinetics ($< \sim 10$ ms, Gutman *et al*., 2005), whereas fast inactivation (N-type inactivation) is probably only seen with $K_v1.4$ and $K_v3.4$ (Gutman *et al*., 2005). Our results may be interpreted in terms of ajmaline preferentially blocking the fast activating and inactivating K_v^+ channels already at lower concentrations (10–25 μM), which is compatible with the strong reduction in peak I_K amplitude observed under prolonged depolarizations (Figure 9b). Larger concentrations ($100\,\mu M$) additionally seem to block other K_v entities as well, thereby strongly reducing steady-state I_K.

Comparing our results to other preparations, ajmaline has been found to block transient outward currents I_{to} in rat ventricular myocytes (Bebarova *et al*., 2005a, b), but also glibenclamide-sensitive K_{ATP} channels in *Xenopus* oocytes (Sakuta *et al*., 1992). In another study, however, expression of cloned cardiac voltage-gated K^+ channels in *Xenopus* oocytes revealed a reduction of potassium currents for several alkaloid drugs tested except for quinidine and ajmaline (Rolf *et al*., 2003), whereas ajmaline reduced currents through cardiac voltage-gated HERG channels in the same expression system (Kiesecker *et al*., 2004).

From the blocking effect on K^+ and Na^+ currents in our study, that is, involving their voltage dependence, we suggest that the S4 subunit could play an important role in binding of ajmaline, to voltage-gated Na^+ and K^+ channels in muscle. In particular, the Hill coefficients, almost equal to unity for both I_{Na} and I_K blocking of ajmaline, suggest a 1:1 stoichiometry of ajmaline to its binding target in both channel entities.

For voltage-gated Na^+ channels, plant alkaloids, including ajmaline, act at six or more distinct receptor sites on the channel protein (Wink, 1993, 2000; Cestele and Catterall, 2000). Further evidence comes from blocking effects of ajmaline on L-type Ca^{2+} currents in ventricular myocytes (Bebarova *et al*., 2005b) and dual effects of prajmaline on Ca^{2+} currents in frog cardiomyocytes (Alvarez and Vassort, 1991). This is expected from the high homology of the voltage-dependent Na^+, K^+ and Ca^{2+} channels (Catterall, 1988; Lehmann-Horn and Jurkat-Rott, 1999). The hypothesis of multiple binding sites is further corroborated by the finding that ajmaline also blocks channels that do not have a voltage sensor (e.g., K_{ATP}). Further research, especially channel modelling and knockout studies will be needed to clarify the exact involvement of the voltage sensors as a target for ajmaline.

Acknowledgements

This work was supported by LFSP 'Biomimetic models of cell mechanics', Baden-Württemberg, Germany. We thank Dr Petra Rohrbach for critical reading of the paper.

Conflict of interest

The authors state no conflict of interest.

References

Almers W, Roberts WM, Ruff RL (1984). Voltage clamp of rat and human skeletal muscle: measurements with an improved loose-patch technique. *J Physiol* **347**: 751–768.

Almers W, Stanfield PR, Stühmer W (1983). Lateral distribution of sodium and potassium channels in frog skeletal muscle: measurement with a patch-clamp technique. *J Physiol* **336**: 261–284.

Alvarez JL, Vassort G (1991). Dual action of prajmaline on the Ca^{2+} currents in frog isolated cardiomyocytes. *J Mol Cell Cardiol* **23**: 627–638.

Beam KG, Donaldson PL (1983). A quantitative study of potassium channel kinetics in rat skeletal muscle from 1 to 37°C. *J Gen Physiol* **81**: 485–512.

Bebarova M, Matejovic P, Pasek M, Simurdova M, Simurda J (2005a). Effect of ajmaline on transient outward current in rat ventricular myocytes. *Gen Physiol Biophys* **24**: 27–45.

Bebarova M, Matejovic P, Pasek M, Simurdova M, Simurda J (2005b). Effect of ajmaline on action potential and ionic currents in rat ventricular myocytes. *Gen Physiol Biophys* **24**: 311–325.

Brugada R, Brugada J, Antzelevitch C, Kirsch GE, Potenza D, Towbin JA *et al.* (2000). Sodium channel blockers identify risk for sudden death in patients with ST-segment elevation and right bundle branch block but structurally normal hearts. *Circulation* **101**: 510–515.

Butterworth JF, Strichartz GR (1990). Molecular mechanisms of local anesthetics: a review. *Anesthesiology* **72**: 711–734.

Caldwell JH, Campbell DT, Beam KG (1986). Na^+ channel distribution in vertebrate skeletal muscle. *J Gen Physiol* **87**: 907–932.

Catterall WA (1988). Structure and function of voltage-sensitive ion channels. *Science* **242**: 50–61.

Catterall WA (1992). Cellular and molecular biology of voltage-gated sodium channels. *Physiol Rev* **72**: S15–S47.

Cestele S, Catterall WA (2000). Molecular mechanisms of neurotoxin action on voltage-gated sodium channels. *Biochimie* **82**: 883–892.

Chen LQ, Santarelli V, Horn R, Kallen RG (1996). A unique role of the S4 segment of domain 4 in the inactivation of sodium channels. *J Gen Physiol* **108**: 549–556.

Desaphy JF, Pierno S, Leoty C, George Jr AL, De Luca A, Camerino DC (2001). Skeletal muscle disuse induces fibre type dependent enhancement of Na^+ channel expression. *Brain* **124**: 1100–1113.

Enomoto K, Imoto M, Nagashima R, Kaneko T, Maruyama T, Kaji Y *et al.* (1995). Effects of ajmaline on non-sodium ionic currents in guinea pig ventricular myocytes. *Jpn Heart J* **36**: 465–476.

Fleishman SJ, Yifrach O, Ben-Tal N (2004). An evolutionary conserved network of amino acids mediates gating in voltage-dependent potassium channels. *J Mol Bol* **340**: 307–318.

Friedrich O, Ehmer T, Fink RHA (1999). Calcium currents during contraction and shortening in enzymatically isolated murine skeletal muscle fibres. *J Physiol* **517**: 757–770.

Friedrich O, Hund E, Weber C, Hacke W, Fink RHA (2004). Critical illness myopathy serum fractions affect membrane excitability and intracellular calcium release in mammalian skeletal muscle. *J Neurol* **251**: 53–65.

Friedrich O, Kress KR, Hartmann M, Frey B, Sommer K, Ludwig H *et al.* (2006). Prolonged high pressure treatments in mammalian skeletal muscle result in loss of functional sodium channels and altered calcium channel kinetics. *Cell Biochem Biophys* **45**: 71–83.

Friedrich O, Kress KR, Ludwig H, Fink RHA (2002). Membrane ion conductances of mammalian skeletal muscle in the post-decompression state after high-pressure treatment. *J Membr Biol* **188**: 11–22.

Gutman GA, Chandy KG, Grissmer S, Lazdunski M, McKinnon D, Pardo LA *et al.* (2005). International Union of Pharmacology. LIII. Nomenclature and molecular relationships of voltage-gated potassium channels. *Pharmacol Rev* **57**: 473–508.

Hamill OP, Marty A, Neher E, Sakmann B, Sigworth FJ (1981). Improved patch-clamp techniques for high-resolution current recording from cells and cell-free membrane patches. *Pflügers Arch* **391**: 85–100.

Hong SJ, Lnenicka GA (1997). Characterization of a P-type calcium current in a crayfish motoneuron and its selective modulation by impulse activity. *J Neurophysiol* **77**: 76–85.

Kalman K, Nguyen A, Tseng-Crank J, Dukes ID, Chandy G, Hustad CM *et al.* (1998). Genomic organization, chromosomal localization, tissue distribution, and biophysical characterization of a novel mammalian shaker-related voltage-gated potassium channel, Kv1.7. *J Biol Chem* **273**: 5851–5857.

Keller DI, Barrane FZ, Gouas L, Martin J, Pilote S, Suarez V *et al.* (2005). A novel nonsense mutation in the SCN5A gene leads to Brugada syndrome and a silent gene mutation carrier state. *Can J Cardiol* **21**: 925–931.

Kiesecker C, Zitrin E, Lück S, Bloehs R, Scholz EP, Kathöfer S *et al.* (2004). Class Ia anti-arrhythmic drug ajmaline blocks HERG potassium channels: mode of action. *Naunyn Schmiedebergs Arch Pharmacol* **370**: 423–435.

Körper S, Wink M, Fink RHA (1998). Differential effects of alkaloids on sodium currents of isolated single skeletal muscle fibres. *FEBS Lett* **436**: 251–255.

Kra-Oz Z, Spira G, Palti Y, Meiri H (1992). Involvement of different S4 parts in the voltage dependency of Na channel gating. *J Membr Biol* **129**: 189–198.

Lehmann-Horn F, Jurkat-Rott K (1999). Voltage-gated ion channels and hereditary disease. *Physiol Rev* **79**: 1317–1372.

Manz M, Mletzko R, Jung W, Luderitz B (1992). Electrophysiological and haemodynamic effects of lidocaine and ajmaline in the management of sustained ventricular tachycardia. *Eur Heart J* **13**: 1123–1128.

McPhee JC, Ragsdale DS, Scheuer T, Catterall WA (1994). A mutation in segment IVS6 disrupts fast inactivation of sodium channels. *Proc Natl Acad Sci USA* **91**: 12346–12350.

McPhee JC, Ragsdale DS, Scheuer T, Catterall WA (1995). A critical role for transmembrane segment IVS6 of the sodium channel alpha subunit in fast inactivation. *J Biol Chem* **270**: 12025–12034.

Pappone PA (1980). Voltage clamp experiments in normal and denervated mammalian skeletal muscle fibres. *J Physiol* **306**: 377–410.

Patel AJ, Lazdunski M, Honore E (1997). Kv2.1/Kv9.3, a novel ATP-dependent delayed rectifier K^+ channel in oxygen-sensitive pulmonary artery myocytes. *EMBO J* **16**: 6615–6625.

PoPa MO, Alekov AK, Bail S, Lehmann-Horn F, Lerche H (2004). Cooperative effect of S4–S5 loops in domains D3 and D4 on fast inactivation of the Na^+ channel. *J Physiol* **561.1**: 39–51.

Ragsdale DS, McPhee JC, Scheuer T, Catterall WA (1994). Molecular determinants of state-dependent block of Na^+ channels by local anesthetics. *Science* **265**: 1724–1728.

Rich MM, Pinter MJ (2003). Crucial role of sodium channel fast inactivation in muscle fibre inexcitability in a rat model of critical illness myopathy. *J Physiol* **547**: 555–566.

Rolf S, Bruns HJ, Wichter T, Kirchhof P, Ribbing M, Wasmer K *et al.* (2003). The ajmaline challenge in Brugada syndrome: diagnostic impact, safety and recommended protocol. *Eur Heart J* **24**: 1104–1112.

Ruff RL (1999). Effects of temperature on slow and fast inactivation of rat skeletal muscle Na(+) channels. *Am J Physiol* **277**: C937–C947.

Sakuta H, Okamoto K, Watanabe Y (1992). Blockade by antiarrhythmic drugs of glibenclamide-sensitive K^+ channels in Xenopus oocytes. *Br J Pharmacol* **107**: 1061–1067.

Stys PK (1995). Protective effects of antiarrhythmic agents against anoxic inury in CNS white matter. *J Cereb Blood Flow Metab* **15**: 425–432.

Thornhill WB, Watanabe I, Sutachan JJ, Wu MB, Wu X, Zhu J *et al.* (2003). Blockade by antiarrhythmic drugs of glibenclamide-sensitive K^+ channels in *Xenopus* oocytes. *J Membrane Biol* **196**: 1–8.

Todt H, Krumpl G, Zojer N, Krejcy K, Raberger G (1993). Effect of ajmaline on sustained ventricular tachycardia induced by programmed electrical stimulation in conscious dogs after myocardial infarction. *Naunyn Schmiedebergs Arch Pharmacol* **348**: 290–297.

Wang SQ, Song LS, Lakatta EG, Cheng H (2001). Ca^{2+} signalling between L-type Ca^{2+} channels and ryanodine receptors in heart cells. *Nature* **410**: 592–596.

Wink M (1993). Allelochemical properties and raison d'être of alkaloids.In: Cordell G. (ed). *The Alkaloids*, vol. 43. Academic Press: New York, pp 1–118.

Wink M (2000). Interference of alkaloids with neuroreceptors and ion channels. In: Atta-Ur-Rahman (ed). *Bioactive Natural Products*, vol. 11. Elsevier: Amsterdam, pp 3–129.

Yao X, Seqal AS, Welling P, Zhang X, McNicholas CM, Engel D *et al*. (1995). Primary structure and functional expression of a cGMP-gated potassium channel. *Proc Natl Acad Sci USA* **92**: 11711–11715.